

PREDICTION OF RAPID DUCTILE CRACK EXTENSION AND ARREST BY AN ANALYTICAL APPROACH

H. J. Schindler
Mat-Tec AG
Winterthur, Switzerland

ABSTRACT

Under special circumstances a fast propagating crack can be triggered in pipelines by just a small local damage. In order to assess the safety with regard to this type of catastrophic failure, an analytical model was established to describe the process of large ductile tearing mathematically. Using a simplifying kinematical model and the hypothesis that the tearing fracture process is governed by a constant CTOA, the total energy dissipation rate can be quantified and compared to the available fracture energy. Since the Charpy fracture energy KV is often the only available toughness-related material parameter of existing pipelines, the toughness parameters used in the model, particularly CTOA, has to be determined from KV. This was achieved by using the same 2-parameter model of ductile tearing to analyse the fracture process in bending. A closed form relationship was obtained between the minimum pressure required for fast ductile crack propagation and the system and material parameters. It could be shown that rapid ductile tearing requires the hoop stress to exceed a certain limit, which depends on the geometrical parameters of the pipeline and KV of its material. The analysis was verified by comparison of the results with the experimental data of full-scale burst tests available in the literature. Unlike empirical correlations, the derived analytical formula seems to be universally valid, regardless of pipe dimensions or steel grades.

INTRODUCTION

A catastrophic mode of failure of a pipeline is the so-called full-bore rupture (FBR), which means the formation of a leak larger than twice the cross section. Such a large leak can be formed by rapid crack propagation in axial direction. The initiation of the crack is usually caused by a local event, such as

“third-party-effect” like denting, or a local overload due to a landslide. However, the subsequent fast crack propagation is no longer influenced or controlled by the triggering event. Its further propagation is autonomous and only a question of whether or not the energy flux to the running crack-tip is sufficient to maintain the required high velocity. If the steel meets the standard toughness requirements and the temperature is not extremely low, the fracture mechanism is ductile tearing, as described in a number of publications, with Refs. [1-8] being only a small selection of them.

Rapid ductile tearing (RDT) can not occur if the fracture toughness of the material is sufficiently high. For this reason, design standards for pipelines such as [9] include requirements in terms of Charpy energy KV. Relations between KV and the crack arrest capability of a pipe are provided by the Battelle 2-curve approach [10] or its simplified version as used in [9]. However, they are mainly based on empirical relations derived from tests and from numerical computations. It is well known that these relations are not universal and cease to give conservative predictions for steel grades higher than X70 [11]. A general analytical model for describing RDT is missing yet.

In the present study the phenomenon of RDT is considered from an analytical point of view. The aim was to describe ductile axial tearing by a transparent model that is simple enough to allow a closed-form solution to be derived, but still capable to capture the key process that govern ductile tearing physically. Since KV is often the only toughness-related material property, the required material parameters such as CTOA should be obtainable from KV, as far as possible. The main theoretical relation between KV and the critical pressure for RDT are already published in [12]. In the present paper, the

derivations are repeated in a slightly different way, but the main emphasis is laid on the discussion of the physical aspects of the model and the analytical results. Compared with [12], some additional experimental data that have been published in the meantime are included in the validation.

DUCTILE TEARING IN GENERAL

In general, ductile tearing of a thin sheet is characterized by the formation of a crack-tip opening angle (CTOA) α , which tends to become constant after a certain minimum distance of crack extension [13]. In a finite body the formation of a finite, macroscopically visible angle α between the crack-faces is only possible, if the entire ligament ahead of the crack is plastically deformed. Two typical load cases of a tearing fracture of an elastic-plastic sheet or plate are sketched in Fig. 1. In the case of a load by parallel displacements between the loaded edges (stretching, Fig. 1a), necking of the fully plastic ligament occurs, with increasing strains on the entire ligament as the crack extends. The fracture is caused by plastic shearing. In the case of a relative rotation between the loaded edges (bending, Fig. 1b), necking is restricted to the region between the centre of rotation and the crack tip, whereas the adjacent part of the ligament suffers plastic swelling due to compression. This causes plastic constraints to the fracture process zone, which manifest fractographically by plastic dimples on the fracture surface. In both cases the energy required for the plastic deformation of the ligament adds to the fracture energy required at the crack tip. Thus, ductile tearing requires a continuous energy input by the external load, which depends on the geometry and the loading case of the cracked body. Under fixed grips conditions, where no external work is supplied, ductile tearing is in general not possible.

According to the energy dissipation rate (EDR) approach [14], tearing crack growth is governed by the equation

$$D_{av} = R_{diss} \quad (1)$$

where D_{av} denotes the available energy per unit crack length, often called the crack driving force (CDF), and R_{diss} the energy dissipation rate (EDR), i.e. the total energy that is dissipated due to crack extension. D_{av} consists of the elastic energy release rate G at the crack-tip according to linear-elastic fracture mechanics (LEFM) and the rate of work supplied by external forces during crack extension, W_{ext} , thus

$$D_{av} = G + \frac{1}{t} \cdot \frac{dW_{ext}}{dc} \quad (2)$$

The second term in (2) is usually much larger than the first one, which represents the elastic energy release rate under fixed grips condition and is given by

$$G = \frac{K_I^2 \cdot (1-\nu^2)}{E} \quad (3)$$

where K_I is the stress intensity factor (SIF).

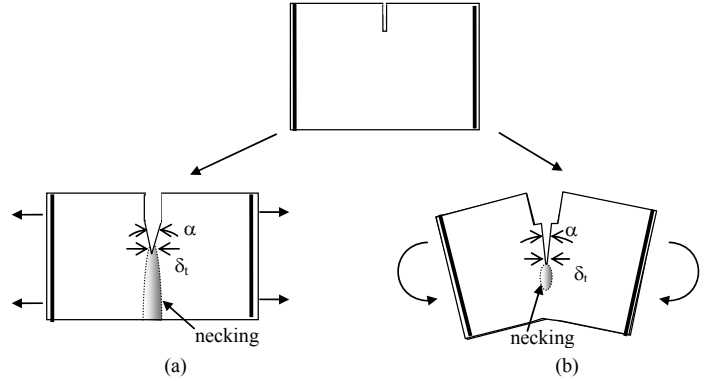


Fig. 1: Definition of crack-tip parameters α and δ_t that are assumed to govern tearing crack growth in a thin plate under stretching (a) and bending (b)

The EDR R_{diss} consists at least of two components as follows:

$$R_{diss} = 2\gamma_p + \frac{1}{t} \cdot \frac{dW_p}{dc} \quad (4)$$

The first term in eq. (4) can be considered as an „effective” surface energy. From basic relations of fracture mechanics it is estimated to be

$$2\gamma_p = \sigma_f \cdot \delta_t \cong \frac{K_{Jd}^2}{E} \quad (5)$$

where δ_t denotes the opening of the blunted crack-tip during crack extension, σ_f the technical flow stress defined as $\sigma_f = (R_{p0.2} + R_m)/2$ and K_{Jd} the upper-shelf fracture toughness under the increased loading rate. The second term in eq. (4) represents the rate of energy consumed by plastic deformation in remote areas of the crack-tip per unit crack extension. It depends on global plastic deformation of the cracking body, so it is not universal, but system-dependent.

ANALYSIS OF AXIAL DUCTILE TEARING IN A PIPE

Ductile tearing in a pipe exhibits several special features compared with ductile tearing in a plane sheet. In order to form a constant CTOA, which is necessary for ductile tearing over a large distance in axial direction, bulging in the wake of the crack is necessary, as can be seen from the example shown in Fig. 2. This requires plastic bending along the baseline of the bulge. The formation of a bulge also requires plastic stretching of the material near the newly formed crack faces in axial

direction. This causes the well-known wrinkling in the wake of the crack (Fig. 3).

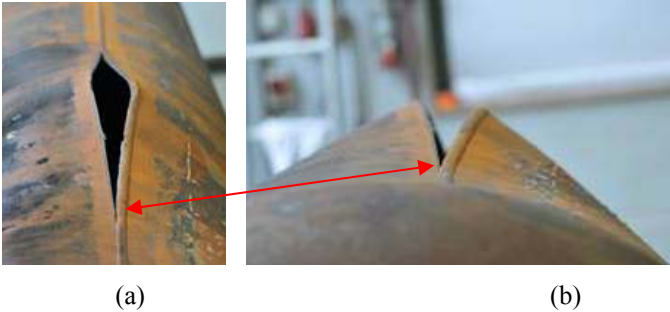


Fig. 2: Example of an axial crack in a pipe due to internal pressure, causing a bulge and the CTOA required for ductile tearing: (a) view in lateral direction, (b) view in axial direction

Another typical feature indicated in Fig. 3 is the flattening of a small area ahead of the pipe ahead of the crack, which appears as a local ovalisation. In the flattened yield zone of length ℓ_p ahead of the crack, necking (i.e. a local reduction of the wall thickness) occurs. Necking starts at the end of the yield zone and is maximal near the crack-tip. However, unlike in the case of a plane fracture as sketched in Fig. 1a, necking is not a continuous process that continuously leads to a shear fracture as the crack tip approaches. It rather has to be regarded as a plastic pre-deformation of the zone that later becomes the fracture process zone. As the crack advances, the fracture process only starts when the necked zone enters into the bulge. The fracture process is restricted to the transition zone between the flattened necking zone and the adjacent region of the bulge. This means that the actual fracture process is restricted to a relatively short range r_p between the bottom of the bulge and the crack-tip, which leads to similar constraints of the process zone as in the case of bending (Fig. 1b). Additional constraints in thickness-direction are caused by the prior necking, which has a similar effect as side-grooves in a fracture mechanics test specimen. This means that constraints in thickness direction are increased, compared with a tearing fracture in a plane sheet. This is the physical reason which RDT fracture surfaces from a RDT-fracture of pipes often exhibit features of relatively high constraints in thickness direction [17, 18]. Therefore, bending-type specimens such as Charpy-V or drop-weight-tear tests (DWTT) reflect the behaviour of a RDT-fracture in a pipe better than plane specimens under tension, such as a wide plate test.

As mentioned above, bulging requires axial stretching of the material next to the crack faces. This gives rise to high axial tensile stresses near the crack tip. This so-called T-stress is known to destabilize the straight crack-path, if the stress is tensile [15, 16]. Thus, straight crack extension in axial direction would not be possible if there was no guidance by the necking formed prior to fracture in the strip-yield zone ahead of the crack. The phenomenon of the lateral deviation of the crack

(“ring-off”) that is often observed just before arrest of RDT (see [7, 17] for example) is explicable by insufficient necking. If the crack propagation slows down below the sonic speed of the medium, necking sufficient to guide the crack in axial direction can no longer be maintained. This explains why RDT often turns into the ring-off behaviour just before it stops.

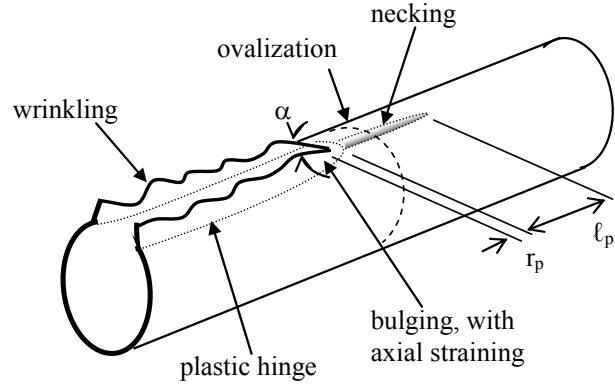


Fig. 3: Special features of a RDT-crack in a pipe

CRACK LOADING AND DRIVING FORCE

As long as the axial crack is relatively short ($c < r$), the SIF of an axial crack of length c in a pipe (Fig. 4) is given by

$$K_I = M_T \cdot \bar{K}_I = M_T \cdot \sigma_t \cdot \sqrt{\pi \cdot c} \quad (6)$$

where

$$\sigma_t = p \cdot r / t \quad (7)$$

M_T denotes the “bulging factor”, which quantifies the increase of K_I compared with the SIF of the same crack in a planar sheet. It results from the circumferential displacements between the crack faces due to the radial displacement in the bulge [19].

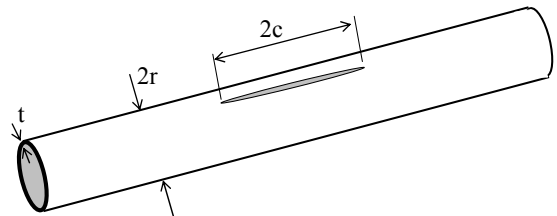


Fig. 4: Definition of geometrical parameters of an axial cracked pipe

In the steady-state situation of a long running crack in an infinitely long pipe, K_I can not depend on crack length c for principal physical reasons. Thus, for cracks longer than a certain saturation-length c_{sat} , both factors appearing in (6),

\bar{K}_I and M_T , will reach a steady-state value that is independent on c . so (6) has to be replaced by

$$K_I(c > c_{sat}) =: K_{I\infty} = M_{T\infty} \cdot \bar{K}_{I\infty} \quad \text{for } c > c_{sat} \quad (8)$$

$\bar{K}_{I\infty}$ is easily obtained from an over-all consideration of the released elastic energy (Appendix A, eq. (A.5)) to be

$$\bar{K}_{I\infty} = \sqrt{G \cdot E} = \frac{P \cdot r^{3/2}}{t} \sqrt{\pi} = \sigma_t \cdot \sqrt{\pi \cdot r} \quad (9)$$

$M_{T\infty}$ for a fast running crack is difficult to be determined analytically or numerically. A comparison of (9) with (6) suggests that $c_{sat} \approx r$. Inserted in the function $M_T(c/r)$ provided in [19], one obtains $M_{T\infty} \approx M_T(c=c_{sat}) \approx 5$. However, this is just a rough estimation. Regarding the difficulties of calculating $M_{T\infty}$ theoretically, it is suitable to consider it as an open constant, which can be determined by adjusting the predictions to experimental results.

$\bar{K}_{I\infty}$ represents the SIF due to the hoop stresses in the pipe, i.e. without the contribution of the radial forces acting in the bulged wake of the crack. Correspondingly, the remaining part of the SIF according to (8),

$$K_{IB} = K_{I\infty} - \bar{K}_{I\infty} = (M_{T\infty} - 1) \cdot \bar{K}_{I\infty} \quad (10)$$

must be due to bulging. These two components of the SIF, $\bar{K}_{I\infty}$ and K_{IB} , should be distinguished, since they play different roles in the fracture process. Particularly, they are decoupled concerning the energy release rate and their contribution to the length of the strip yield zone, ℓ_p . The latter only depends on the component $\bar{K}_{I\infty}$ of the SIF, since the effect of bulging, quantified by K_{IB} , can hardly spread out in axial direction beyond the baseline of the bulge. ℓ_p can be estimated by Dugdale's model [20] to be

$$\ell_p = \frac{\pi}{8} \cdot \frac{\bar{K}_{I\infty}^2}{\sigma_f^2} = \frac{\pi^2 \cdot \sigma_t^2}{8 \cdot \sigma_f^2} \cdot r \quad (11)$$

The corresponding component of the energy release rate,

$$G = -\frac{1}{t} \cdot \frac{dU_{el}}{dc} = \frac{K_{I\infty}^2}{E}, \quad (12)$$

delivers the required energy for the plastic deformation in the strip yield zone and for the necking therein. The energy release rate corresponding to K_{IB} ,

$$G_B = \frac{K_{IB\infty}^2}{E} (1 - \nu^2) = \frac{(M_{T\infty} - 1)^2 \bar{K}_{I\infty}^2}{E} (1 - \nu^2) = \frac{1}{t} \cdot \frac{dW_{ext}}{dc}, \quad (13)$$

represents the energy per unit crack extension that is available for the tearing process in the near-tip region of the bulge. G_B is the rate of work done by the pressure on the radial displacements of the near-tip bulge. Thus, as indicated in eq. (13), G_B can be interpreted as the second term in (2), so CDF becomes

$$D_{av} = G + G_B = \frac{\pi \cdot P^2 \cdot r^3}{E \cdot t^2} (1 - \nu^2) \cdot (2 - 2M_{T\infty} + M_{T\infty}^2) \quad (14)$$

Note that the formal use of relations of LEFM, such as in (12) or (13), is not restricted to a relatively small plastic zone, as long as the latter is stationary. Actually, the derivation in Appendix A is valid for any length of the plastic zone ℓ_p , including $\ell_p \gg r$. Although the SIF may be fictive (i.e not measurable from the stresses in the vicinity of the crack because of excessive plasticity), quantities like G or ℓ_p calculated by (11) – (13) still have their correct physical meanings.

ENERGY DISSIPATION RATE

As shown by the example in Fig 2 and by the sketch in Fig. 3, a tearing crack extension in axial direction in a pipe is associated with plastic deformation in radial direction. The corresponding energy dissipation contributes substantially to the EDR. To estimate this contribution in quantitative terms, the upper limit theorem of the theory of plasticity is adapted. A possible, kinematically admissible mode of deformation to form the CTOA α between the crack faces is shown in Fig. 5(b): To produce a crack prolongation increment Δc under a given angle α , the crack flanks have to be bent upwards by a rotation angle β along a linear hinge, which occurs under an unknown angle γ with respect to the axial direction. The energy dissipated in the corresponding linear plastic hinge due to a crack extension Δc is found to be

$$\Delta W_p = \frac{c_d \cdot \sigma_f \cdot t^2 \cdot \beta}{2 \cdot \cos \gamma} \cdot \Delta c \quad (15)$$

with

$$\beta = \arccos \left(1 - \frac{\tan \frac{\alpha}{2}}{\sin \gamma \cdot \cos \gamma} \right) \quad (16)$$

The factor c_d is introduced to account for the increase of σ_f due to the high loading rate associated with rapid crack extension. Its value is estimated to be in the order of 1.5.

Since W_p as given by eq. (15) represents an upper bound of the “real” dissipated energy, the decisive hinge orientation γ

is the one that minimizes $W_p(\gamma)$. This is the case for $\gamma=30^\circ$. With $\gamma=30^\circ$ and $dW_p/dc = \Delta W_p/\Delta c$, one obtains from eq. (5), (15) and (16)

$$R_{diss} = \frac{K_{Jc}^2}{E} + \frac{c_d \cdot \sigma_f \cdot t}{\sqrt{3}} \cdot \arccos\left(1 - \frac{2}{\sqrt{3}} CTOA_{tan}\right) \quad (17)$$

where $CTOA_{tan}$, which is defined as

$$CTOA_{tan} = 2 \cdot \tan(\alpha/2), \quad (18)$$

is introduced as a non-dimensional parameter to quantify the physical CTOA α .

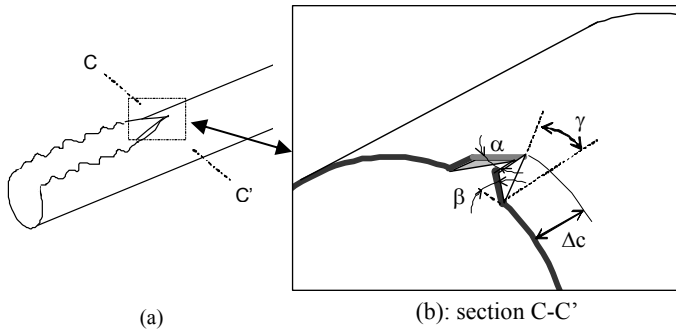


Fig. 5: Axial tearing crack in a pipe (a), with model of the deformation mechanism in the vicinity of the crack-tip (b).

Actually, (17) only covers the near-tip contribution to the total dissipated energy, i.e. the energy associated with the deformation shown as the local part (section C-C') in Fig. 5. During RDT there is additional plastic deformation going on, such as plastic straining in axial direction and wrinkling in remote regions of the crack faces, as shown in Fig. 3. Correspondingly, although derived from an upper limit analysis, eq. (17) is expected to be a rather conservative lower bound of the actual dissipated energy per unit crack extension.

CRITERION FOR RAPID DUCTILE TEARING

Inserting (14) and (17) in the governing equation (1) leads to the following criterion for RDT:

$$\sigma_t \geq \sigma_{RDT} \quad (19a)$$

where

$$\sigma_{RDT} = \sqrt{\frac{0.175 \cdot K_{Jd}^2 + 0.151 \cdot \sigma_f \cdot t \cdot E \cdot \arccos\left(1 - 1.15 \cdot CTOA_{tan}\right)}{r \cdot \left(1 - M_{T\infty} + \frac{M_{T\infty}^2}{2}\right)}} \quad (19b)$$

The material properties K_{Jd} and $CTOA_{tan}$ have to be determined experimentally. There are several empirical

relations to estimate K_{Jd} from the Charpy fracture energy. It is suggested to use

$$K_{Jd} [N/mm^{1.5}] \cong \sqrt{\frac{7.33 \cdot A_g [\%] \cdot KV [J] \cdot E [MPa]}{\left(100 - 147 \cdot \frac{KV [J]}{R_m [MPa]}\right) \cdot (1 - \nu^2)}} \quad (20)$$

which is derived in [21] semi-empirically and validated independently in [22].

Concerning $CTOA_{tan}$, it is advisable to determine it analytically from the fracture energy of a bending test by using the analogous model of tearing as in the analysis of the crack in a pipe, rather than to measure it optically. By using basically the same analytical model, the inaccuracies that result from the corresponding simplifications tend to compensate each other. As shown in Appendix B, the 2-parameter tearing model that was used to obtain (17) enables a relation between $CTOA_{tan}$ and the total fracture energy of a test specimen to be derived. The application of (B.6) to a standard Charpy V-notch specimen ($B = 10$ mm, $b_0 = 8$ mm, $\rho = 0.25$ mm) and assuming $c_d=1.5$, $c_m=1.4$ delivers

$$CTOA_{tan} = \frac{2.98 \cdot KV}{\sigma_f} \cdot \left(1 - \frac{A_g [\%]}{100}\right) - \frac{0.238 \cdot K_{Jd}^2}{\sigma_f \cdot E} - 0.0625 \quad (21)$$

where K_{Jd} shall be inserted in $N/mm^{1.5}$, KV in J , σ_f and E in MPa .

Due to the appearance of A_g both in (20) and (21), σ_{RDT} according to (19b) becomes only weakly dependent on A_g . This means that there is no need for A_g to be known precisely; a rough estimate is sufficient. Unless the actual value is known from a measurement, we recommend to use 20% for a low-strength steel, 15% for a medium strength steel and 10% for a high strength steel.

As discussed above, the bulging factor $M_{T\infty}$ in (19b) can be determined by adjusting (19) - (21) to experimental results of full scale burst tests. For the sake of conservatism $M_{T\infty}$ should be chosen such that the hoop stresses that led to crack propagation in the tested pipes are higher than those predicted by (19). This means that in the representation of Fig. 6 all the full symbols should be located right from the dashed line, as they do for $M_{T\infty} = 5$. Fig. 6 includes test data obtained on pipes of various steel qualities in the range from X65 to X100. Obviously, all the experimental results are covered in a conservative way by this choice of $M_{T\infty}$.

Eqs. (19) - (21) can be solved for the design-factor DF , which is defined as $DF = \sigma_t/R_{p0.2}$, as a function of the Charpy energy KV required to prevent RDT. As examples, two common types of pipelines used in Switzerland are considered

in Fig. 7. For these materials, $KV > 40$ J is specified. Thus, the allowable design factors for these pipes, denoted in Fig. 7 as DF_I and DF_{II} , can be determined from the limit curves shown in Fig. 7 at $KV = 40$ J to be about $DF_I = 0.49$ for pipe type I and $DF_{II} = 0.44$ for type II. For comparison: For the same pipes and $KV = 40$ J the requirements according to “Alternative 2” in [9] lead to allowable design factors of $DF_I = 0.91$ and $DF_{II} = 0.54$. This comparison indicates that the presented model tends to be more conservative for steel grades lower than those included in the comparisons shown Fig. 6.

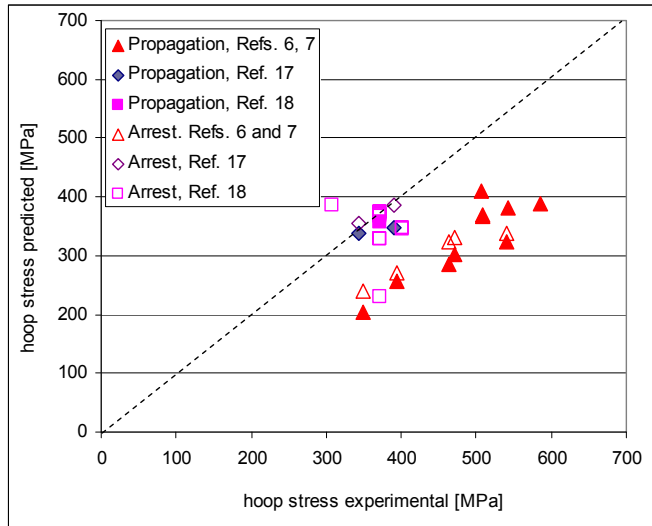


Fig. 6: Comparison of experimental hoop stress of full-scale burst tests data from [6, 7, 17, 18] with predictions from (19)-(21) with $M_{T\infty} = 5$.

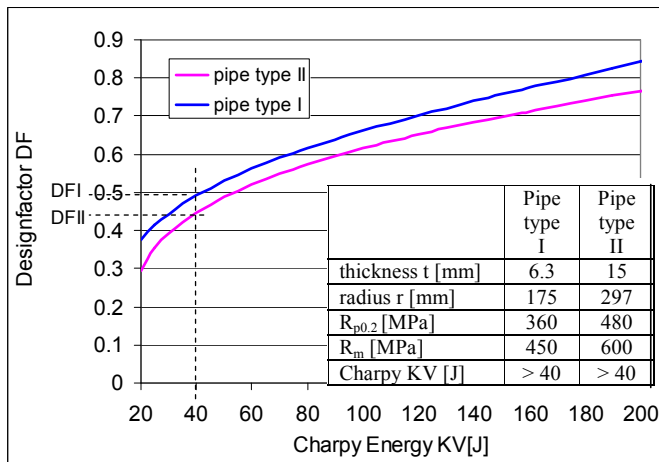


Fig. 7: Minimum design factor $DF = \sigma_t / R_{p0.2}$ to enable rapid ductile tearing as a function of KV, shown by examples of two types of pipes common for gas transportation in Switzerland.

DISCUSSION AND CONCLUSIONS

By the presented model, which reflects the relevant physical mechanisms of axial crack propagation in a pipe by tearing, a mathematical equation in closed form could be derived to quantify the condition that need to be fulfilled for

RDT to occur. It can be expressed as a critical pressure p_{RDT} or a critical hoop stress σ_{RDT} as a function of the pipe dimensions, the material’s yield strength and its toughness. If the hoop stress stays below this critical value, RDT is not possible for energetic reasons.

Concerning the toughness, CTOA is shown to be the most relevant parameter. CTOA is known to depend on the constraint condition of the test specimen. As discussed above, the constraints in a RDT in a pipe are similar to those in bending. Therefore, bending tests of relatively small specimens are more adequate to determine CTOA than tensile tests of a plate. It is preferable to determine CTOA analytically from a fracture test in bending by using the same 2-parameter model as in the analysis of RDT in the pipe, rather than to measure it explicitly by optical means. Charpy tests are suitable for this purpose. Instrumented Charpy tests on pre-cracked specimens would be preferable.

Regarding quantitative predictions, the bulging factor $M_{T\infty}$ plays a key role in eq. (19b). Being difficult to be determined analytically or numerically, it is appropriate to determine it by comparison with full-scale test data. It was found that with $M_{T\infty} = 5$ all the available test data were covered in a conservative way, whereas $M_{T\infty} = 4$ leads to rather realistic predictions. Note that $M_{T\infty} \approx 5$ corresponds to the rough theoretical estimation explained above. This means that the presented model enables relatively good predictions to be made. This remarkable performance, which is unequalled by any other purely theoretical approach known so far, confirms the present simple model and the underlying assumptions.

However, the main advantage of an analytical approach is its capability to identify the key influencing parameters and to show their effects on the results quantitatively. Since the model is general, with no empirical factors or assumptions involved, there is no reason why arbitrary pipes should behave different from the ones that have been used to validate the model. Therefore the presented relations are expected to hold universally, for any pipe dimension and steel grades, probably even all kinds of elastic-plastic materials.

Concerning the physics of RDT it was recognized that the necking that takes place in the plastic zone in front of the crack plays an important role in guiding the crack along the axial direction. Without a sufficient necking – which can occur if the crack extension rate is insufficient to avoid decompression in front of the crack-tip - the crack path becomes unstable due to the positive T-stress, so the crack tends to deviate laterally from the straight line. This leads to the well-known “ring-off” that often takes place prior to crack arrest.

In recent literature, DWTT-testing is often considered to be better suited than the classical Charpy test to characterize the resistance against RDT. However, from the present analysis

it is not clear whether or not this is true. As discussed in the second section above, the plastic constraints at the fracture process zone in a pipe are different from the ones in a DWTT-specimen, even if the thickness is the same. Concerning crack-tip constraints, out-of-plane bending plays an important role in the tearing mechanism of an axial crack in a pipe. This can not be reproduced correctly by in plane bending anyway, neither by Charpy- nor by DWTT-testing. The aspect of transferability needs further consideration.

In the present analysis it was assumed that the pipeline is free, i.e. without backfill. If it is embedded in the soil, then additional energy is dissipated by compression of the soil. The latter results from the radial displacements of the pipe, which is associated with large ductile tearing crack extension, as shown in the present analysis. The corresponding energy dissipation per unit crack extension adds to R_{diss} as given by eq. (17), leading to an increase of σ_{RDT} in eq. (19b). Thus, as expected, the surrounding soil increases the critical value of the hoop stress for RDT to occur, or decreases the required Charpy energy to prevent RDT, respectively.

NOMENCLATURE

A_g	standard uniform fracture strain (in %)
c	half crack length
$CTOA_{tan}$	non-dimensional CTOA as defined in eq. (18)
D_{av}	Available energy per unit crack extension
DF	design factor, defined as $DF = \sigma_t/R_{p0.2}$
E	Young's modulus
G	Energy release rate
$K_{I\infty}$	K_I for a crack longer than the saturation value
K_{Jd}	fracture toughness under increased loading rate
KV	Charpy fracture energy
l_p	length of plastic zone
M_T	bulging factor
$M_{T\infty}$	Bulging factor for a crack longer than the saturation value
p	internal pressure
r	pipe radius
R_{diss}	Dissipated energy per unit crack extension
R_m	ultimate tensile stress
r_p	length of fracture process zone
$R_{p0.2}$	yield stress
t	pipe wall thickness
W_{ext}	Work done by external forces
α	crack tip opening angle (in deg)
β	angle as defined in Fig. 5
γ	angle as defined in Fig. 5

γ_p	fracture energy per unit crack area
δ_t	crack tip opening displacement
σ_f	technical flow stress, $\sigma_f = (R_{p0.2} + R_m)/2$
σ_{RDT}	stress required for rapid ductile tearing
σ_t	hoop stress in pipe
CDF	crack driving force
CTOA	crack tip opening angle
EDR	energy dissipation rate
FBR	full bore rupture
KV	Fracture energy in standard Charpy test
LEFM	linear-elastic fracture toughness
RDT	rapid ductile tearing
SIF	stress intensity factor

ACKNOWLEDGMENT

This study was sponsored by SWISSGAS, Zürich. The author wishes to thank Dr. M. Harzenmoser for his support.

REFERENCES

- [1] Maxey, W. A., et al., Ductile fracture initiation, propagation, and arrest in cylindrical vessels. In *ASTM STP 514, 1971*
- [2] Rudland, D.L., Wikowski, G, et al., „Determination of conditional probability of dynamic ductile axial crack arrest for linepipe materials“, J. Pressure Vessel technology, Vol. 127, 2005, 143-150,
- [3] Cosham, A., and Hopkins, P., The pipeline defect assessment manual, Proceedings of IPC 2002: International Pipeline Conference 2002, Calgary, Alberta, Canada
- [4] Rosenfeld, M.J., Technology procedure improves line pipe Charpy test interpretation, Oil & Gas Journal, Vol. 95, 1997
- [5] Mannucci, G., et al., X-100 Fracture initiation and propagation, Proceeding of 1st Conf. Super High Strength Steel, SHSS, Ed. AIM Italy, Rome, Italy, Nov. 2005, Paper 175.
- [6] O'Donoghue, P.E., et al., The development and validation of a dynamic fracture propagation model for gas transmission pipelines, Int. J. Pressure Vess. and Piping, Vol. 70, 1996, 11-25
- [7] Takeuchi, I., et al., Crack arrest ability of high pressure gas pipelines by X100 or X120, 23rd World Gas Conference, Amsterdam 2006
- [8] Rothwell, A.B., The Application of the Battelle „Short Formula“ to the determination of ductile fracture arrest toughness in gas pipelines“, Pipeline Conference, Vol. 1, ASME, 2000, 233 – 238
- [9] PrEN ISO 3183:2005, Stahlrohre für Rohrleitungs-transportssysteme, Appendix G (2005)

- [10] PRCI Report No. PR-003-00108, Fracture control technology for natural gas pipelines; Eiber, R.J. and Leis, B.N., July 2001
- [11] Erdelen-Peppler, M., Hillenbrand, H.-G., and Knauf, G., Limits of existing crack arrest models, Pipeline Technology Conference, Ostend, 12-14 October 2009, Paper No. 2009-116
- [12] Schindler, H.J., An analytical model to estimate the crack arrest capability of a pipeline from the Charpy fracture energy, Proc. 12th Int. Conf. on Fracture, 2009, Ottawa
- [13] Newman, J.C., et al., A review of the CTOA/CTOD fracture criterion, Eng. Fracture Mechanics, 70, 2003, 371-385
- [14] Sumpster, J.D.G., Size Effects in tearing instability: An analysis based on energy dissipation rate, Eng. Fract. Mechanics, 74, 2007, 2352-2374
- [15] Cotterell, B., Rice, J.R., Int. J. Fracture, Vol. 16, 1980, 155 - 169
- [16] Schindler, H.J., Sayir, M., Path of a crack in a beam due to dynamic flexural fracture, Int. Journal of Fracture, Vol. 25, p. 95 - 107, 1984,
- [17] Tagawa T, Igi S, and Kawaguchi S, Fractography of pipeline burst tests, Pipeline Technology Conference, Ostend, 12-14 October 2009, Paper No. 2009-021
- [18] Pyshmintsev, I Y., et al., Crack arrestability and mechanical properties of 1420mm X80 Grade pipes designed for 11.8MPa operation pressure, Pipeline Technology Conference, Ostend, 12-14 October 2009, Paper No. 2009-078
- [19] Kiefner, J.F., et al., Failure Stress Levels of Flaws in pressurized cylinders, ASTM STP 536, 1973, 461-481
- [20] Dugdale, D.S., Yielding of steel sheets containing slits, J. Mechanics and Physics of Solids, 8, 1960, p. 100
- [21] Schindler, H.J., "Relation Between Fracture Toughness and Charpy Fracture Energy - An Analytical Approach", ASTM STP 1380, T. Siewert and M. P. Manahan, Sr., Eds., ASTM, West Conshohocken, PA, 1999, 337-353
- [22] Sreenivasan, P.R., Moitra, A., Ray, S.K., Mannan, S.L., Predicting reference temperature from instrumented Charpy V-notch impact tests using modified Schindler procedure for computing dynamic fracture toughness Int. J. Fracture, 125, 387-403, 2004

A. CALCULATION OF $K_{I\infty}$

Consider a pipe of radius r , wall thickness t and length $2L$ with an axial crack of length $2c$, (Fig. A.1). It is divided in 3 regions I, II and III, where d , which represents the half length of region II, is constant and the same order of magnitude as r .

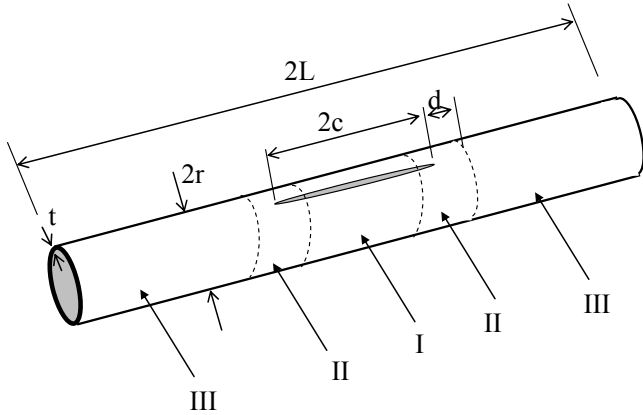


Fig. A.1: Pipe with axial crack of length $2c$, with regions I, II and III

ANNEXES

The total elastic energy stored in the pipe is

$$U_e = U_{eI} + 2U_{eII} + 2U_{eIII} \quad (A.1)$$

where U_{eI} , U_{eII} and U_{eIII} are the amounts of elastic energy stored in the corresponding areas of the pipe indicated in Fig. A.1, thus

$$U_{eI} = 0 \quad (A.2)$$

$$U_{eIII} = \frac{\pi \cdot r^3 \cdot p^2}{E \cdot t} \cdot (L - c - d) \quad (A.3)$$

U_{eII} can not be given in a simple formula, but for $c \gg r$ and $L - c \gg r$

$$\frac{\partial U_{eII}}{\partial c} = 0 \quad (A.4)$$

With (A.1) – (A.4) the energy release rate G

$$G = -\frac{1}{t} \cdot \frac{\partial U_e}{\partial c} \quad (A.4)$$

is obtained to be

$$G = \left(\frac{p \cdot r}{t} \right)^2 \cdot \frac{\pi \cdot r}{E} \quad (A.5)$$

By the general relation $K_I = \sqrt{G \cdot E}$ one obtains

$$K_t = \left(\frac{P \cdot r}{t} \right) \cdot \sqrt{\pi \cdot r} \quad (\text{A.6})$$

B. ESTIMATION OF CTOA FROM AN IMPACT BENDING TEST

Consider an arbitrary 3-point bending test on a notched or pre-cracked specimen, for example a Charpy-V- test (Fig. B.1). Provided the force-displacement (F-s-) diagram is known - as in the case of an instrumented Charpy test - the total fracture energy KV can be split in the initiation energy W_{mp} and the tearing energy W_t as shown in Fig. B.2. As derived in [21], W_t can be calculated by (see Fig. B.3):

$$W_t = KV - W_{mp} = \int_{b_0}^0 M(b) \cdot d\vartheta(b) \quad (\text{B.1})$$

with

$$M(b) = \frac{c_d \cdot c_m}{4} \sigma_f \cdot B \cdot b^2 \quad (\text{B.2})$$

where c_m is introduced as a factor to account for the constraints in a ligament in bending under essentially plane strain, which is known to be about 1.4. The factor c_d is introduced to account for the increase in flow stress due to the strain rate. It can be assumed to be about 1.5 for a Charpy test. For kinematical reasons (see Fig. B.3)

$$d\vartheta(b) = -\frac{CTOA_{\tan}}{z \cdot b} db - \frac{\delta_t}{(z \cdot b)^2} db \quad (\text{B.3})$$

where $z \cdot b$ denotes the distance between the centre of rotation and the crack tip. Approximatly, it can be assumed that $z \approx 0.5$. $CTOA_{\tan}$ is defined in eq. (18). δ_t is the opening displacement at the actual crack tip. It can be estimated from a basic relation of LEFM to be

$$\delta_t = \frac{K_{Jc}^2}{c_m \cdot c_d E \cdot \sigma_f} \quad (\text{B.4})$$

where K_{Jd} is the upper shelf fracture toughness under increased loading rates, which can be estimated from KV by the well known empirical correlations or by eq. (20).

In the case of a classical Charpy test the F-s-diagram is not available. As shown in [21] W_{mp} can be estimated by

$$W_{mp} \cong \frac{A_g [\%]}{100} \cdot KV + \frac{1}{2} c_d \cdot c_m \cdot \sigma_f \cdot b_0 \cdot B \cdot \rho \quad (\text{B.5})$$

The first term in eq. (B.5) holds for a pre-cracked specimen [20]. The second represents the additional energy required to initiate a crack at the blunt notch of a Charpy specimen, which has a root radius of $\rho = 0.25$ mm. Combining eqs. (B.1 – B.5) leads to

$$CTOA_{\tan} = \frac{\left[KV \cdot \left(1 - \frac{A_g [\%]}{100}\right) - \frac{1}{2} c_d \cdot c_m \cdot \sigma_f \cdot b_0 \cdot B \cdot \rho \right] \cdot 8z}{B \cdot \sigma_f \cdot c_d \cdot c_m \cdot b_0^2 - \frac{2 \cdot K_{Jc}^2}{z \cdot b_0 \cdot \sigma_f \cdot c_d \cdot c_m \cdot E}} \quad (\text{B.6})$$

The physical CTOA is obtained from (B.6) by (18) as

$$\alpha = 2 \arctan \left(\frac{CTOA_{\tan}}{2} \right) \quad (\text{B.7})$$

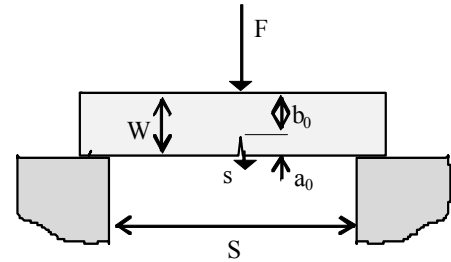


Fig. B.1: Mechanical system of an impact bending test

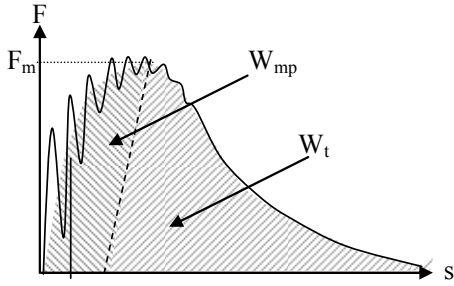


Fig. B.2: Force-deflection-(F-s-) diagram of impact bending test or Charpy test

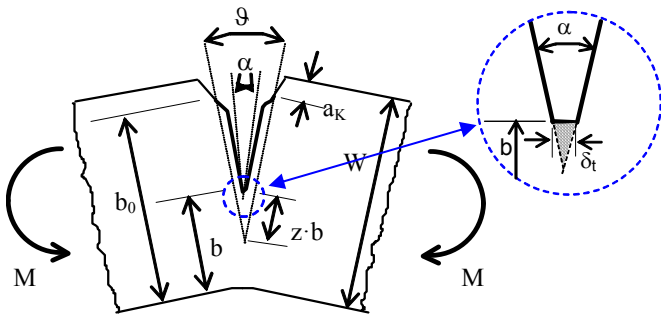


Fig. B.3: Tearing crack growth model (Fig. 1) applied to a fracture test in bending